ENVIRONMENTAL RESEARCH
COMMUNICATIONS

ACCEPTED MANUSCRIPT • OPEN ACCESS

Unexpected high contribution of in-cloud wet scavenging to nitrogen deposition induced by pumping effect of typhoon landfall in China

To cite this article before publication: tan qixin *et al* 2023 *Environ. Res. Commun.* in press https://doi.org/10.1088/2515-7620/acb90b

IOP Publishing Journal Title
Journal **XX** (XXXX) XXXXXX https://doi.org/XXXX/XXXX

Unexpected high contribution of in-cloud wet scavenging to nitrogen deposition induced by pumping effect of typhoon landfall in China

Qixin Tan[1,2], Baozhu Ge[1*], Syuichi Itahashi[3],Lu Gan[4], Ying Zhang[1], Shuyan Xie[5], Ying Liu[6], Danhui Xu[7], Xueshun Chen[1], Lin Wu[1], Xiaole Pan[1], Wei Wang[8], Jianbin Wu[9], Jie Li[1], Junhua Wang[1,2], Xiaobin Xu[10], Joshua S. Fu[11], Zifa Wang[1,2]

[1] State Key Laboratory of Atmospheric Boundary Layer Physics and Atmospheric Chemistry, Institute of Atmospheric Physics, Chinese Academy of Sciences, Beijing 100029, China
[2] University of Chinese Academy of Sciences, Beijing, 100049, China
[3] Sustainable System Research Laboratory, Central Research Institute of Electric Power Industry (CRIEPI), Abiko, Chiba 270–1194, Japan
[4] Beijing Weather Forecast Center, Beijing, 100089, China
[5] State Environmental Protection Key Laboratory of Quality Control in Environmental Monitoring, China National Environmental Monitoring Centre, Beijng 100012, China
[6] Laboratory for Climate Studies & CMA-NJU Joint Laboratory for Climate Prediction Studies, National Climate Center, China Meteorological Administration, Beijing, China
[7] National Center for Climate Change Strategy and International Cooperation, Ministry of Ecology and Environment, Beijing 100035, China
[8] National center for environmental quality forecast, CNEMC, 100012, Beijing
[9] Clear Technology Co. Ltd, Beijing 100029, China
[10] Key Laboratory for Atmospheric Chemistry, Chinese Academy of Meteorological Sciences, Beijing, China
[11] Department of Civil and Environmental Engineering, University of Tennessee, Knoxville, TN 37996, USA

Correspondence author: Baozhu Ge (gebz@mail.iap.ac.cn)

IOP Publishing Journal Title
Journal **XX** (XXXX) XXXXXX https://doi.org/XXXX/XXXX

Abstract

Atmospheric nitrogen deposition has large eco-environmental effects such as ocean acidification, eutrophication in coastal areas. However, knowledge of the source and the pathway of N deposition in coastal areas is limited, especially during tropical storms, hindering the accurate quantification of how anthropogenic activities influence the ocean ecosystem. In this study, the Nested Air Quality Prediction Modeling System was used to investigate the wet deposition of N induced by typhoon Hagupit over eastern coastal China from an in- and below-cloud process perspective. Our results reveal for the first time an enhancement mechanism of N deposition related to the 'pumping effect' of the typhoon. Different from the non-typhoon conditions, air pollutants in the typhoon-affected regions were pumped into the higher altitudes and deposited via the in-cloud scavenging process in the moving path of the typhoon-affected regions. This study updates our understanding of the source–receptor relationship on atmospheric wet deposition caused by tropical cyclones.

Keywords: in-cloud scavenging, wet deposition, source–receptor relationship, typhoon

1. Introduction

Atmospheric nitrogen (N) deposition has important eco-environmental effects, including acid rain (Du, 2018; Page et al., 2008), corrosion of buildings (Knotkova & Barton, 1992), ocean acidification (Doney et al., 2007), nutrient anomalies (Hao et al., 2011) and biodiversity reduction (Pitcairn et al., 2003). The economic development in the country around the Chinese inland sea and North Pacific Ocean has resulted in gradually increasing level of the nutrient concentration such as dissolved inorganic nitrogen (DIN), turning these oceanic regions into nitrogen-rich basins. Statistically, atmospheric N deposition has been proven to be a larger contributor to the DIN input into the ocean than the riverine input, providing 10%–40% of the N in N-limited coastal regions (Okin et al., 2011; J. Zhang et al., 1999). Wang et al. (2019) estimated that about 25.81% of the total DIN input in the Yellow Sea and Bohai Sea derives from the atmospheric N deposition. The contribution of N deposition from China reported by Ge et al. (2014) and Kajino et al. (2013) is about 40%–60% and 51%–76%.

Typhoons usually carry associated hazards, such as strong winds, storm surges, and rainfall, which can cause considerable damage and disruption. In addition to these direct forms of damage, the wet deposition of nitrogen caused by typhoons, which also serves as a lager contributor of DIN, has also drawn much attention in coastal regions (Chen et al., 2015; Fang et al., 2009; Lin et al., 2000; Sakihama & Tokuyama, 2005; Toyonaga & Zhang, 2016; Yan et al., 2016; Tan et al., 2018), especially against the background of global climate change, which has resulted in an increased frequency and intensity of typhoons over the past two decades (Bender et al., 2010; Knutson et al., 2010; Webster et al., 2006). Lin et al. (2000) reported that wet deposition caused by typhoons represented 20% of the total deposition based on three years of observations in a subtropical rainforest in Taiwan. Toyonaga and Zhang (2016) conducted continuous field measurements of wet deposition fluxes of ions at a coastal site in Japan from 1996 to 2003 and estimated an N wet deposition flux rate associated with typhoons of 1 meq m^{-2} yr^{-1}. To a certain extent, these studies help us to understand the wet deposition of N caused by typhoons.

As we know, the wet deposition is governed by two main processes: in-cloud scavenging and below-cloud scavenging (Ge et al., 2014; Santachiara et al., 2012; Seinfeld & Pandis, 2016; Xu et al., 2017; 2019). For strong convective system (cold vortexes/typhoon), in-cloud contributions of inorganic nitrogen (IN) wet deposition are higher than thought, achieving 82% during continuous observations from 2013 to 2017 (Ge et al., 2021). This reveals that the study on the source-receptor (S/R) of IN wet deposition during the typhoons should focus on the source of in-cloud IN wet deposition. However, knowledge of the source and pathway of N deposition by model simulation in coastal areas remains limited. Previous studies on the S/R relationship of deposition (Holloway et al., 2002; Kajino et al., 2013; Kajino et al., 2011; Lin et al., 2008), as well as multi-model comparisons (e.g., MICS-Asia III, HTAP II) (Ge et al., 2020; Tan et al., 2018), were able to quantitatively investigate the source of total wet deposition via sensitivity experiments but not in-cloud wet deposition. The sensitivity experiments to obtain the S/R of deposition inevitably introduce nonlinear errors caused by the changes in emission sources (Grewe, 2004). Besides, these S/R relationship of IN deposition during non-typhoon period could not be applicate to that during typhoon due to different air conditions caused by typhoon (Chiang et al., 2005; Fang et al., 2009). This indicates the S/R relationships of N wet deposition during deep convective process of the typhoon, especially the source and pathway of N deposition should be explored to help us to improve the knowledge of the new mechanism of typhoon induced wet deposition.

In this study, we carried out simulations of the wet deposition of inorganic N (IN) during typhoon Hagupit (3–6 August 2020) induced by in- and below-cloud scavenging using the Nested Air Quality Prediction Modeling System (NAQPMS) (Wang et al., 2001) coupled with the online tracer tagging method. Based on the simulation results, the influence of the typhoon on the wet deposition of IN, especially the in-cloud wet deposition in eastern China, is discussed. Besides, the source contributions of the in- and below-cloud wet deposition with the movement of the typhoon after it made landfall in the Yangtze River Delta (YRD) were quantified. The purpose of this study is to update our knowledge on the S/R relationships of in- and below-cloud wet deposition in typhoon-affected regions and explore the new mechanism of influence of typhoons on wet deposition.

2. Materials and Methods

2.1. Model description and setup

NAQPMS is a 3-D Eulerian terrain-following air quality model, which is developed by Wang et al. (2001). It has been widely used to simulate the air pollutants, such as ozone (Li et al., 2011; 2016), dust (Tian et al., 2020), anthropogenic aerosols (Chen et al., 2017; Du et al., 2019; Wang et al., 2017; Yang et al., 2018), and even toxic pollutants like mercury (Chen et al., 2015), as well as the sulfur and nitrogen wet depositions over China (Ge et al., 2014). Recently, NAQPMS has been invited to participate in the Model Inter-Comparison Study for Asia III (MICS-Asia III) to compare the simulated air pollutants (Kong et al., 2020; Li et al., 2019) as well as the depositions (Ge et al., 2020; Itahashi et al., 2020) over East Asia among 14 regional and global air

quality models. In this study, the cloud processes schemes for in-cloud scavenging (Dennis et al., 1993; Ge et al., 2014) and the below-cloud scavenging scheme (Xu et al., 2017; 2019; 2020) have been updated in NAQPMS to better simulate the wet deposition of air pollutants. In order to investigate the S/R of wet deposition of IN, an online tracer tagging module is also implemented in NAQPMS to track the formation and evolution of air pollutants (Li et al., 2008; Wu et al., 2017). Unlike other studies that can only track the source of the total wet deposition (Kajino et al., 2013; Lin et al., 2008), NAQPMS coupled with the on-line tracer tagging module can quantitatively estimate the S/R of the below- and in-cloud wet deposition without introducing errors by nonlinear chemistry. Further technical details about the NAQPMS can be found in Text S1-S2 and in Li et al, (2011;2013;2016) and Ge et al. (2014).

The model domain covers the East Asia (15.4°S-58.3°N, 48.5°-160.2°E), which is set on a Lambert conformal map projection with 180×170 grids at 45 km horizontal resolution. Vertically, the numerical model has 20 terrain-following layers from the surface to the height of 20 km with the lowest 10 layers below 3 km. The global atmospheric chemical transport model MOZART v2.4 provided initial and lateral boundary conditions for the NAQPMS. The meteorological fields for NAQPMS were provided by the Weather Research and Forecasting (WRF) model, version 3.4.1 (Skamarock et al., 2008) driven by National Centers for Environmental Prediction Final Analysis reanalysis data (1° × 1°). More detailed descriptions of the WRF model including the Physics schemes can refer to in Text S3 and in Ge et al. (2021). Emissions for NAQPMS are obtained from the emissions inventory in MICS-Asia III (Li et al., 2017), and considering the yearly projections of the variations through the satellite-constrained NO_x and ammonia (NH_3) emissions based on vertical column density (VCD) values in 2020. More detailed descriptions of the updated emission can be found in Text S4. The model's output of IN wet deposition can be classified as oxidized N (N_{ox}), including particulate nitrate, gaseous nitrate acid and NO_x, and reduced N (N_{rd}) including NH_3 and particulate ammonium. The simulation period was from 24 July to 6 August 2020, with 8 days of model spin-up time from 24 to 31 July 2020.

Figure S1 shows 22 identified areas (ID) in the NAQPMS model simulation domain. Fifteen land areas in the territory of China (i.e., YRD, FJ, SD, NCP, SX, HN, AH, HB, JX, SW, TW, West, Middle, NW, and NE) are marked in different colors, together with North Korea (NK), South Korea (SK) and Japan. The three major oceanic regions along the pathway of typhoon Hagupit (green line depicted in Figure S1) are marked as ECS (East China Sea), WP (West Pacific), and JS (Japan Sea), respectively. The definitions of the 22 IDs are listed in Table S1.

2.2. Observational data

Ground-based observations of wet deposition collected at sites shown in Figure 1a-c during 1–6 August 2020 by the China National Environmental Monitoring Centre (CNEMC) (http://www.cnemc.cn) and Acid Deposition Monitoring Network in East Asia (EANET)) (http://www.eanet.asia/, last access date: 25 June 2022) were used to validate the performance of the model with respect to the wet deposition of N_{ox} and N_{rd}. Six of 48 stations are in SW, 9 in HN, 8 in SD, 11 in YRD, 4 in West, 4 in FJ, 2 in Middle, 1 in WP, 2 in Japan and 1 in SX (Table S2). The CNEMC observations of wet deposition included daily average inorganic ion concentrations (SO_4^{2-}, NO_3^-, NH_4^+, F^-, Cl^-, Ca^{2+}, Mg^{2+}, Na^+, and K^+) and daily accumulated precipitation from 1 to 6 August 2020. Because CNEMC sites mainly covered inland China, EANET sites located in coastal area over East Asia is additionally analyzed in this study (More information about the EANET observation can refer to Ge et al., (2020)). After quality control (Text S5), the measured anion and cation concentrations of precipitation samples from 48 stations were nearly in balance and there were no large deficiencies of major inorganic ions. Surface observations of hourly $PM_{2.5}$ and NO_2 concentrations at the 48 stations from 1–6 August 2020 were also used in this study. Ground meteorological observations of daily precipitation and wind were obtained from China Meteorological Administration. The best-track data of typhoon Hagupit provided by the Japan Meteorological Agency were used to identify the location of the typhoon (https://www.jma.go.jp/jma/jma-eng/jma-center/rsmc-hp-pub-eg/besttrack.html, last access: 16 December 2021).

2.3. Model validation

The NAQPMS was able to simulate the precipitation and wet deposition of IN both in typhoon-affected regions and in the other regions of China. The simulated accumulated precipitation in the typhoon-affected region during the pre-landfall (1–2 August), landfall (3–4 August), and post-landfall (5–6 August) stages shows good correlation, with a correlation coefficient (R) of 0.79 (N=11), 0.78 (N=110) and 0.75 (N=92), and normalized mean bias (NMB) of −19%, −12.6% and 12.7%, respectively (Figure 1d-1f). In the S-high control region, the R values are 0.66 (N=48), 0.64 (N=41) and 0.68 (N=45) for the pre-landfall, landfall and post-landfall stages, respectively, and the NMB values are −19.5%, 17.6% and −9.1% (Figure S2a-b). Compared to the reported statistical scores in MICS-Asia III (Itahashi et al., 2020; Ge et al., 2020), our modeling performance in this study have been confirmed as better. In accordance with the good model performance for precipitation, the simulated wet deposition of IN agrees well with the observations, with the NMB ranging from −25% to +2% (Figure 1d-i). At stations

IOP Publishing Journal Title
Journal **XX** (XXXX) XXXXXX https://doi.org/XXXX/XXXX

in the typhoon-affected region especially YRD, the simulated wet deposition values of N_{ox} and N_{rd} are very close to their observed counterparts, with NMBs of 4% and 8%, respectively. At stations in the S-high control region, the wet deposition of N_{ox} was overestimated by the model, with an NMB of +32%. Such positive bias in the simulated IN wet deposition is mainly due to the overestimation of N precursors, up to +20% for NO_x as reported by Ge et al. (2020).

3. Results

3.1. Typhoon track and typhoon-affected regions

As the track of Hagupit in Figure 1b (blue lines) shows, the typhoon impacted eastern China after it made landfall in the YRD on 3 August. According to the MODIS true-color image taken on 3 August (Figure S3a), the location of mostly the cloud-free typhoon eye overlaps with the typhoon position at 00:00 UTC on 3 August. Then, the typhoon continued to move in a northeasterly direction after it entered the Bohai Sea. Finally, it made landfall in SK. The model performance of typhoon track simulation is important to reproduce the structure of typhoon surface precipitation and cloud hydrometeors (Chavas & Emanuel, 2010; Hong et al., 2020; Irish et al., 2008; Kumar et al., 2020; Merrill, 1984). Besides the well-simulated precipitation by WRF, the typhoon track was also consistent with that obtained from Japan Meteorological Agency (Text S3 and Figure S4). The whole typhoon track can be divided into three stages, as Figure 1a-c show, i.e., the pre-landfall stage (1–2 August), the landfall stage (3–4 August), and the post-landfall stage (5–6 August).

3.2. Pumping effect of the typhoon

Figure S5 shows latitude–height cross-sections of the ratio of the $PM_{2.5}$ concentration to that at ground level with the vertical wind vector superimposed. More than 30%–49% of the $PM_{2.5}$ concentration at ground level could be lifted to altitudes higher than 2–3 km in less than 10 hours. All cross-sections over the landfalling regions of the typhoon simulated by NAQPMS captured these fast and violent uplifts of $PM_{2.5}$. The gaseous precursor of nitrate and ammonium, NO_x, and NH_3 in the same cross-sections, were also found to be uplifted to high altitudes within a very short time (Figure 2 and 3). In particular, NO_x was strongly lifted to as high as about 4 km altitudes (Figure 2c) due to the strong upward winds in the typhoon, while the lifting of NH_3 was significantly weaker than that of NO_x and $PM_{2.5}$. This is reasonable that NH_3 is mainly emitted by agricultural sources (e.g., livestock and synthetic fertilizers) located on the surface (Aneja et al., 2003), whereas NO_x pollution occurs primarily through emissions from the industry at higher altitudes, for example, stack chimney emission (Aneja et al., 2001). The higher altitude the emission source is, the easier for the pollutants to be uplifted to a higher altitude and hence the more contribution to long-range transport.

Vertical transport of air pollutants can be caused by different mechanisms. Boundary layer turbulent mixing can contribute to the vertical transport of pollutants, but it is limited by the boundary layer height (0.6–0.8 km). The cold-front structure of most cyclones can also lift pollutants to 1–2.5 km above the ground (Kang et al., 2019). However, only very strong cyclones such as typhoons may lift air pollutants to almost double the high altitudes that most cyclones can. This indicates that pollutants in the surface layer, such as $PM_{2.5}$ and NO_x, were quickly lifted to altitudes higher than 2–3 km when typhoon Hagupit made landfall. This elevation of pollutants influenced by the typhoon is hereafter referred to as the typhoon's 'pumping effect' (Figure 4).

3.3. Contributions from in- and below-cloud scavenging

In order to illustrate the influence of the 'pumping effect', wet deposition of IN from in-cloud and below-cloud fractions was recorded by NAQPMS. The typhoon-affected regions in YRD as well as the precipitation region in Shanxi province affected by subtropical anticyclone (hereafter called S-high) are selected to compare the different mechanisms of IN wet deposition. The definition of the S-high region is followed by He et al. (2015), who use the 5880m geopotential height at 500 hPa to relate with the S-high regions as shown in Figure S6, and hence was displayed as the blue rectangle in Figure 1.

Box plots of the below- and in-cloud wet deposition and their contributions to the total wet deposition of N_{ox} and N_{rd} during the pre-landfall, landfall, and post-landfall stages in the YRD and S-high region are displayed in Figure 5. In YRD, with the average precipitation increasing from 5.6 to 21.6 mm, the in-cloud N_{ox} wet deposition contribution changed from 75% during pre-landfall to 89% during landfall. In the S-high region, however, in-cloud N_{ox} wet deposition contribution increased only slightly from 63% to 67%, with the average precipitation increasing from 14 to 27.6 mm. A similar phenomenon is found for N_{rd} wet deposition. Xu et al. (2017) pointed out that the in-cloud contributions to the total wet deposition will increase with the increase in rainfall as the effect of the washout process weakens. However, the increase of in-cloud contributions is limited by the concentrations of pollutants within the clouds. The larger increase in the typhoon-affected region than in the S-high region indicates the significance of the typhoon's 'pumping effect', which elevates the surface air pollutants to high altitudes and contributes more to the in-cloud scavenging during precipitation events. It is noteworthy that the upper limit of the in-cloud contribution of N_{ox} (N_{rd}) reached 89% (80%) during the typhoon, which is

significantly higher than the average value of 39% (53%) in 2014 observed in China (Xu et al., 2017) and the value of 34% observed in Japan (Aikawa & Hiraki, 2009; Aikawa et al., 2014). The highest value (82%) was found in the cold vortex events during the four years observation in Beijing, China reported by Ge et al. (2021). This observation confirms that in-cloud contributions for strong convective weather systems like typhoons and cold vortexes can be much higher than thought (Figure 6; Figure S7).

3.4. Source identification into the scavenging pathways

To better characterize the mechanism of nitrogen deposition induced by typhoons, detailed simulations were done using the updated NAQMPS. Different from the previous studies, the source of wet deposition during the typhoon event was firstly identified in relation to wet scavenging processes (Figure 7). Three typical typhoon-affected regions, i.e., YRD, Bohai, and SK were chosen as the receptor regions under the influence of typhoon Hagupit to quantitatively investigate the source of in- and below-cloud wet deposition.

For the YRD, the largest source contribution to the in-cloud wet deposition in the YRD was from local emission (Table S3), accounting for 52% (38%) of the in-cloud wet deposition of N_{ox} (N_{rd}). The relative contribution to the below-cloud from YRD was 68% (48%), corresponding up to 8% (9%) of total wet depositions of N_{ox} (N_{rd}). This reveals that local emissions were the dominant source of both in-cloud and below-cloud wet deposition in the YRD. For Bohai, the largest contribution was from emissions in the YRD, reaching up to 47% of the total wet deposition of N_{ox}, which was about four times higher than other sources (Table S3). However, pollutants from the YRD contributed significantly less to the in-cloud wet deposition of N_{rd} than that of N_{ox} (1.5 vs. 7.2×10^{-3} mg m^{-2} h^{-1}, Table S3). For SK, the largest in-cloud contributor was also from the YRD. However, the largest contributor to the total wet deposition of N_{ox} in SK was the local emission, which accounted for 32% of the total wet deposition, with 5% from the below-cloud part. Detailed analysis of the S/R relationship in three regions can be found in Text S6 and Table S3.

Analysis of IN deposition caused by typhoons in terms of scavenging pathways can shed light on typhoons' effect on the coastal region, optimize the source identification and help to protect the marine ecological environment. This updated S/R relationship of in-cloud wet deposition during the typhoon event challenges the traditional view that the in-cloud wet deposition of acidic pollutants is mainly linked with medium- or long-range transport, which is mainly in non-typhoon events. This significantly higher contribution from the YRD region can be attributed to the 'pumping effect' of the typhoon, which influenced greatly not only the long-range transport of IN from the YRD to Bohai and SK but also the local wet deposition in the YRD itself.

3.5. Implications to the knowledge of IN wet deposition affected by typhoon landfall

What will the mechanism so-called "pumping effect" of typhoon affect the wet deposition of nitrogen in the downwind typhoon-affected regions. We have quantified the effect of the "pumping effect" according to the S/R relationship of N_{ox} wet deposition as Figure 4 shows. As section 3.2 described, when typhoon HAGUPIT made landfall in YRD, the $PM_{2.5}$ and NO_x in the multiple cross-sections, were found to be uplifted to higher than 2-3 km in less than 10 hours due to deep convective transports associated with cyclones (Fadnavis, S et al., 2011). These pollutants were scavenged by the clouds, making the in-cloud wet deposition significant increase in this study.

According to Table S3, when typhoon made landfall in YRD, 106 $x10^{-3}$ mg m^{-2} amount of oxidized N were uplifted into the cloud by the pumping effect of typhoon. Meanwhile, with the development of rainfall in YRD, 37 $x10^{-3}$ mg m^{-2} of uplifted N from YRD were scavenged by in-cloud process, which accounts for 52% of the total wet deposition in YRD (a). With the movement of typhoon, the remained amount of 69 $x10^{-3}$ mg m^{-2} oxidized N pollutants (g) induced by pumping effect were transported into downwind typhoon-affected regions such as Bohai and South Korea. This made 7.2 $x10^{-3}$ mg m^{-2} in-cloud wet deposition of N_{ox} (c) in Bohai and 42 $x10^{-3}$ mg m^{-2} in-cloud wet deposition of N_{ox} (e) in South Korea. Different from the in-cloud scavenging, the below-cloud scavenging was much smaller. Almost $6x10^{-3}$ mg m^{-2} amounts of oxidized N from local region were washed out and deposited into YRD (b). Due to the airflow supported by typhoon, $5x10^{-3}$ mg m^{-2} amounts of oxidized N from YRD (h) were transported below the cloud to downwind areas such as Bohai (0.4 $x10^{-3}$ mg m^{-2}) and South Korea (<$1x10^{-3}$ mg m^{-2}).

The contributions of long-range transport from the YRD were almost maintained above 40% in Bohai and 30% in SK mainly via the in-cloud process. This means that, as the typhoon moved to downwind areas, the long-range transport of pollutants from the YRD constantly influenced the in-cloud wet deposition in Bohai and SK. The largest source contribution to the in-cloud wet deposition in the YRD was local, which contributed to 52% of the in-cloud wet deposition of N_{ox}. This reveals that local emissions were the dominant source of the in-cloud wet deposition in the YRD. This updated S/R relationship of in-cloud wet deposition during this typhoon event challenges the traditional view that, the in-cloud wet deposition of acidic pollutants is mainly linked with medium- or long-range transport. The above analysis reveals the importance of contributions from emissions in typhoon landing to the typhoon-affected regions.

This mechanism of wet deposition due to the 'pumping effect' may have profound effects on the wet deposition of N in typhoon-affected areas.

4. Conclusions

The updated wet scavenging module in NAQPMS, coupled with the online tracer tagging method, was used to investigate the sources of in- and below-cloud N wet deposition during the landfall of typhoon Hagupit in the YRD, China. The model was able to capture the observed variations of N_{ox} and N_{rd} during the movement of Hagupit. Based on the NAQPMS simulations as well as the observations, the influence of the so-called 'pumping effect' mechanism of the typhoon on the wet deposition of N was explored. This made the air pollutants easy for them to be captured by cloud droplets and deposited via the in-cloud scavenging process, which contributed to 80%–89% of the wet deposition of N in the typhoon-affected region. In addition, the present study has improved our knowledge of the S/R relationship of the wet deposition of N during the landfall stage of typhoons in China, especially the in- and below-cloud processes of wet deposition. As the landfall region for Hagupit, the YRD was found to be the largest contributor of wet deposition via the in-cloud process, not only for itself but also in the other regions of Hagupit's pathway, i.e., the Bohai Sea and South Korea. This can be attributed to the 'pumping effect', which contributes to a large proportion of the in-cloud wet deposition in the downwind typhoon-affected regions. Continuous observations of wind profile radar combined with aircraft data show that the vertical wind profile and intensity of pressure are of crucial importance for determining a tropical cyclone's radial inflow (Liao et al., 2019). This means that the amounts of pollutants which typhoon pumps into are closely related to model simulation of the intensity of the typhoon itself. The simulation of intensity pressure of typhoon, especially the central pressure does not reach the actual observation. The error caused by the typhoon simulation of air pressure could affect the model performance on pumping volume. Fujita et al., (2004) observed the inflow height would get stronger as typhoon moved to north-eastward. Probably, with typhoon moving north-eastward the height of 'pumping effect' can reach beyond the 2-3 km, which was found in this study, and this uncertainty will further lead to uncertainty in the amount of in-cloud scavenging, long-range transport and the deposition. Besides, improving the model performance of the central pressure of typhoon should also be considered in future. Also, different typhoons would have multiple and variable height of "pumping effect", which should been examined with typhoon moving north-east.

Data availability statements

All data including observation data and NAQPMS simulation results used for the figures are publicly available at https://doi.org/10.5281/zenodo.5227241.

References

Aikawa, M., & Hiraki, T. (2009). Washout/rainout contribution in wet deposition estimated by 0.5 mm precipitation sampling/analysis. *Atmospheric Environment, 43*(32), https://doi.org/10.1016/j.atmosenv.2009.07.057

Aikawa, M., Kajino, M., Hiraki, T., & Mukai, H. (2014). The contribution of site to washout and rainout: Precipitation chemistry based on sample analysis from 0.5 mm precipitation increments and numerical simulation. *Atmospheric Environment, 95*, https://doi.org/10.1016/j.atmosenv.2014.06.015

Aneja, V. P., Nelson, D. R., Roelle, P. A., Walker, J. T., & Battye, W. (2003). Agricultural ammonia emissions and ammonium concentrations associated with aerosols and precipitation in the southeast United States. *Journal of Geophysical Research-Atmospheres, 108*(D4), https://doi.org/10.1029/2002jd002271

Aneja, V. P., Roelle, P. A., Murray, G. C., Southerland, J., Erisman, J. W., Fowler, D., et al. (2001). Atmospheric nitrogen compounds II: emissions, transport, transformation, deposition and assessment. *Atmospheric Environment, 35*(11), https://doi.org/10.1016/s1352-2310(00)00543-4

Bae, S. Y., Jung, C. H., & Kim, Y. P. (2009). Relative contributions of individual phoretic effect in the below-cloud scavenging process. *Journal of Aerosol Science, 40*(7), https://doi.org/10.1016/j.jaerosci.2009.03.003

Bender, M. A., Knutson, T. R., Tuleya, R. E., Sirutis, J. J., Vecchi, G. A., Garner, S. T., & Held, I. M. (2010). Modeled impact of anthropogenic warming on the frequency of intense Atlantic hurricanes. *Science, 327*(5964), https://doi.org/10.1126/science.1180568

Bertrand, G., Celle-Jeanton, H., Laj, P., Rangognio, J., & Chazot, G. (2009). Rainfall chemistry: long range transport versus below cloud scavenging. A two-year study at an inland station (Opme, France). *Journal of Atmospheric Chemistry, 60*(3), https://doi.org/10.1007/s10874-009-9120-y

Cai, K., Li, S. S., Zheng, F. B., Yu, C., Zhang, X. Y., Liu, Y., & Li, Y. J. (2018). Spatio-temporal Variations in NO2 and PM2.5 over the Central Plains Economic Region of China during 2005-2015 Based on Satellite Observations. *Aerosol and Air Quality Research, 18*(5), https://doi.org/10.4209/aaqr.2017.10.0394

Chavas, D. R., & Emanuel, K. A. (2010). A QuikSCAT climatology of tropical cyclone size. *Geophysical Research Letters, 37*(18), https://doi.org/10.1029/2010gl044558

Chen, H., Wang, Z., Li, J., Tang, X., ge, B., Wu, X., et al. (2015). GNAQPMS-Hg v1.0, a global nested atmospheric mercury transport model: model description, evaluation and application to trans-boundary transport of Chinese anthropogenic emissions. *Geoscientific Model Development, 8*, https://doi.org/10.5194/gmd-8-2857-2015

Chen, X., Wang, Z., Yu, F., Pan, X., Li, J., ge, B., et al. (2017). Estimation of atmospheric aging time of black carbon particles in the polluted atmosphere over central-eastern China using microphysical process analysis in regional chemical transport model. *Atmospheric Environment, 163*, https://doi.org/10.1016/j.atmosenv.2017.05.016

Chen, Y. X., Chen, H. Y., Wang, W., Yeh, J. X., Chou, W. C., Gong, G. C., et al. (2015). Dissolved organic nitrogen in wet deposition in a coastal city (Keelung) of the southern East China Sea: Origin, molecular composition and flux. *Atmospheric Environment, 112*, https://doi.org/10.1016/j.atmosenv.2015.04.023

Chiang, P. C., Chang, E. E., Chang, T. C., & Chiang, H. L. (2005). Seasonal source-receptor relationships in a petrochemical industrial district over northern Taiwan. *J Air Waste Manag Assoc*, *55*(3), 326-341. https://doi.org/10.1080/10473289.2005.10464625

Cho, S., Park, H., Son, J., & Chang, L. (2021). Development of the Global to Mesoscale Air Quality Forecast and Analysis System (GMAF) and Its Application to PM2.5 Forecast in Korea. *Atmosphere, 12*(3), https://doi.org/10.3390/atmos12030411

Dennis, R. L., McHenry, J. N., Barchet, W. R., Binkowski, F. S., & Byun, D. W. (1993). Correcting RADM's sulfate underprediction: Discovery and correction of model errors and testing the corrections through comparisons against field data. *Atmospheric Environment. Part A. General Topics, 27*(6), https://doi.org/https://doi.org/10.1016/0960-1686(93)90012-N

Doney, S. C., Mahowald, N., Lima, I., Feely, R. A., Mackenzie, F. T., Lamarque, J. F., & Rasch, P. J. (2007). Impact of anthropogenic atmospheric nitrogen and sulfur deposition on ocean acidification and the inorganic carbon system. Proc Natl Acad Sci U S A, 104(37), 14580-14585.https://www.ncbi.nlm.nih.gov/pubmed/17804807

Du, E. (2018). A database of annual atmospheric acid and nutrient deposition to China's forests. Sci Data, 5(1), 180223. https://www.ncbi.nlm.nih.gov/pubmed/30325353

Du, H. Y., Li, J., Chen, X. S., Wang, Z. F., Sun, Y. L., Fu, P. Q., et al. (2019). Modeling of aerosol property evolution during winter haze episodes over a megacity cluster in northern China: roles of regional transport and heterogeneous reactions of SO2. *Atmospheric Chemistry and Physics, 19*(14), https://doi.org/10.5194/acp-19-9351-2019

Fadnavis, S., Beig, G., Buchunde, P., Ghude, S. D., & Krishnamurti, T. N. (2011). Vertical transport of ozone and CO during super cyclones in the Bay of Bengal as detected by Tropospheric Emission

Spectrometer. Environ Sci Pollut Res Int, 18(2), 301-315. https://doi.org/10.1007/s11356-010-0374-3

Fang, G. C., Lin, S. J., Chang, S. Y., & Chou, C. C. K. (2009). Effect of typhoon on atmospheric particulates in autumn in central Taiwan. *Atmospheric Environment, 43*(38), https://doi.org/10.1016/j.atmosenv.2009.08.033

Fowler, D., Pitcairn, C. E. R., Sutton, M. A., Flechard, C., Loubet, B., Coyle, M., & Munro, R. C. (1998). The mass budget of atmospheric ammonia in woodland within 1 km of livestock buildings. *Environmental Pollution, 102*(1), https://doi.org/10.1016/s0269-7491(98)80053-5

Fujita, H., Teshiba, M., Umemoto, Y., Shibagaki, Y., Hashiguchi, H., Yamanaka, M., & Fukao, S. (2004). Study on the extratropical transition of typhoon 0310 (Etau) observed by wind profilers and weather radars. Proceedings of ERAD

Ge, B., Itahashi, S., Sato, K., Xu, D., Wang, J., Fan, F., et al. (2020). Model Inter-Comparison Study for Asia (MICS-Asia) phase III: multimodel comparison of reactive nitrogen deposition over China. *Atmospheric Chemistry and Physics, 20*, https://doi.org/10.5194/acp-20-10587-2020

Ge, B., Itahashi, S., Sato, K., Xu, D., Wang, J., Fan, F., et al. (2020). MICS-Asia III Multi-model comparison of reactive Nitrogen deposition over China. *Atmos Chem Phys*, https://doi.org/10.5194/acp-2019-1083

Ge, B. Z., Wang, Z. F., Gbaguidi, A. E., & Zhang, Q. X. (2016). Source Identification of Acid Rain Arising over Northeast China: Observed Evidence and Model Simulation. *Aerosol and Air Quality Research, 16*(6), https://doi.org/10.4209/aaqr.2015.05.0294

Ge, B. Z., Wang, Z. F., Xu, X. B., Wu, J. B., Yu, X. L., & Li, J. (2014). Wet deposition of acidifying substances in different regions of China and the rest of East Asia: modeling with updated NAQPMS. *Environ Pollut, 187*, https://doi.org/10.1016/j.envpol.2013.12.014

Ge, B. Z., Xu, D. H., Wild, O., Yao, X. F., Wang, J. H., Chen, X. S., et al. (2021). Inter-annual variations of wet deposition in Beijing from 2014-2017: implications of below-cloud scavenging of inorganic aerosols. *Atmospheric Chemistry and Physics, 21*(12), https://doi.org/10.5194/acp-21-9441-2021

Grewe, V. (2004). Technical Note: A diagnostic for ozone contributions of various NO_x emissions in multi-decadal chemistry-climate model simulations. *Atmospheric Chemistry and Physics, 4*(3), https://doi.org/10.5194/acp-4-729-2004

Hao, Y. J., Tang, D. L., Yu, L., & Xing, Q. G. (2011). Nutrient and chlorophyll a anomaly in red-tide periods of 2003-2008 in Sishili Bay, China. Chinese Journal of Oceanology and Limnology, 29(3), 664-673.

He, C., Zhou, T., Lin, A., Wu, B., Gu, D., Li, C., & Zheng, B. (2015). Enhanced or Weakened Western North Pacific Subtropical High under Global Warming? *Sci Rep, 5*(1), https://doi.org/10.1038/srep16771

Holloway, T., Levy, H., & Carmichael, G. (2002). Transfer of reactive nitrogen in Asia: development and evaluation of a source-receptor model. *Atmospheric Environment, 36*(26), https://doi.org/10.1016/S1352-2310(02)00316-3

Hong, W., Zheng, Y. L., Chen, B., Su, T. H., & Ke, X. Q. (2020). Monthly variation and spatial distribution of quadrant tropical cyclone size in the Western North Pacific. *Atmospheric Science Letters, 21*(2), https://doi.org/10.1002/asl.956

Huang, X., Song, Y., Li, M., Li, J., Huo, Q., Cai, X., et al. (2012). A high-resolution ammonia emission inventory in China. *Global Biogeochemical Cycles, 26*(1), https://doi.org/10.1029/2011gb004161

Institute), K. K. E. (2008). *Korea Environmental Policy Bulletin:Korea Environment Institute, Republic of Korea: Emission Reduction Program for In-Use Diesel Vehicles* Retrieved from https://wedocs.unep.org/bitstream/handle/20.500.11822/9050/-Korea%20Environmental%20Policy%20Bulletin%20-%20Emission%20Reduction%20Program%20for%20In-Use%20Diesel%20Vehicles-2008Emission%20Reduction%20Program%20for%20In-Use%20Diesel%20Vehicles_KEPB2008.pdf?sequence=3&isAllowed=y

Irish, J. L., Resio, D. T., & Ratcliff, J. J. (2008). The influence of storm size on hurricane surge. *Journal of Physical Oceanography, 38*(9), https://doi.org/10.1175/2008jpo3727.1

Itahashi, S., Ge, B., Sato, K., Fu, J. S., Wang, X., Yamaji, K., et al. (2020). MICS-Asia III: overview of model intercomparison and evaluation of acid deposition over Asia. Atmospheric Chemistry and Physics, 20(5), https://doi.org/10.5194/acp-20-2667-2020

Izquierdo, R., Avila, A., & Alarcon, M. (2012). Trajectory statistical analysis of atmospheric transport patterns and trends in precipitation chemistry of a rural site in NE Spain in 1984-2009. *Atmospheric Environment, 61*, https://doi.org/10.1016/j.atmosenv.2012.07.060

Kajino, M., Sato, K., Inomata, Y., & Ueda, H. (2013). Source-receptor relationships of nitrate in Northeast Asia and influence of sea salt on the long-range transport of nitrate. *Atmospheric Environment, 79*, https://doi.org/10.1016/j.atmosenv.2013.06.024

Kajino, M., Ueda, H., Sato, K., & Sakurai, T. (2011). Spatial distribution of the source-receptor relationship of sulfur in Northeast Asia. *Atmospheric Chemistry and Physics, 11*(13), https://doi.org/10.5194/acp-11-6475-2011

Kang, H. Q., Zhu, B., Gao, J. H., He, Y., Wang, H. L., Su, J.

F., et al. (2019). Potential impacts of cold frontal passage on air quality over the Yangtze River Delta, China. *Atmospheric Chemistry and Physics, 19*(6), https://doi.org/10.5194/acp-19-3673-2019

Knotkova, D., & Barton, K. (1992). Effects of Acid Deposition on Corrosion of Metals. *Atmospheric Environment*. Part a-General Topics, 26(17), 3169-3177. https://doi.org/10.1016/0960-1686(92)90473-X

Knutson, T., Landsea, C., & Emanuel, K. (2010). Tropical Cyclones and Climate Change: A Review. In *Global Perspectives on Tropical Cyclones* (pp. 243-284).

Kong, L., Tang, X., Zhu, J., Wang, Z., Fu, J., Wang, X., et al. (2020). Evaluation and uncertainty investigation of the NO_2, CO and NH_3 modeling over China under the framework of MICS-Asia III. *Atmospheric Chemistry and Physics, 20*, https://doi.org/10.5194/acp-20-181-2020

Kumar, S., Panda, J., Singh, K., Guha, B. K., & Kant, S. (2020). Structural characteristics of North Indian Ocean tropical cyclones during 1999–2017: a scatterometer observation-based analysis. *Theoretical and Applied Climatology, 143*(1-2), https://doi.org/10.1007/s00704-020-03431-w

Kurokawa, J., Ohara, T., Morikawa, T., Hanayama, S., Janssens-Maenhout, G., Fukui, T., et al. (2013). Emissions of air pollutants and greenhouse gases over Asian regions during 2000–2008: Regional Emission inventory in ASia (REAS) version 2. *Atmospheric Chemistry and Physics, 13*(21), https://doi.org/10.5194/acp-13-11019-2013

Lachatre, M., Fortems-Cheiney, A., Foret, G., Siour, G., Dufour, G., Clarisse, L., et al. (2019). The unintended consequence of SO2 and NO2 regulations over China: increase of ammonia levels and impact on PM2.5 concentrations. *Atmos. Chem. Phys., 19*(10), https://doi.org/10.5194/acp-19-6701-2019

Lee, D., Lee, Y.-M., Jang, K.-W., Yoo, C., Kang, K.-H., Lee, J.-H., et al. (2011). Korean National Emissions Inventory System and 2007 Air Pollutant Emissions. *Asian Journal of Atmospheric Environment, 5*(4), https://doi.org/10.5572/ajae.2011.5.4.278

Li, J., Wang, Z., Akimoto, H., Yamaji, K., Takigawa, M., Pochanart, P., et al. (2008). Near-ground ozone source attributions and outflow in central eastern China during MTX2006. *Atmospheric Chemistry and Physics, 8*(24), https://doi.org/10.5194/acp-8-7335-2008

Li, J., Wang, Z., Wang, X., Yamaji, K., Takigawa, M., Kanaya, Y., et al. (2011). Impacts of aerosols on summertime tropospheric photolysis frequencies and photochemistry over Central Eastern China. *Atmospheric Environment, 45*(10)

Li, J., Wang, Z., Huang, H., Hu, M., Meng, F., Sun, Y., et al. (2013). Assessing the effects of trans-boundary aerosol transport between various city clusters on regional haze episodes in spring over East China. *Tellus B: Chemical and Physical Meteorology, 65*(1), https://doi.org/10.3402/tellusb.v65i0.20052

Li, J., Yang, W. Y., Wang, Z. F., Chen, H. S., Hu, B., Li, J. J., et al. (2016). Modeling study of surface ozone source-receptor relationships in East Asia. *Atmospheric Research, 167*, https://doi.org/10.1016/j.atmosres.2015.07.010

Li, J., Nagashima, T., Kong, L., Ge, B., Yamaji, K., Fu, J., et al. (2019). Model evaluation and intercomparison of surface-level ozone and relevant species in East Asia in the context of MICS-Asia Phase III – Part 1: Overview. *Atmospheric Chemistry and Physics, 19*, https://doi.org/10.5194/acp-19-12993-2019

Li, M., Zhang, Q., Kurokawa, J.-i., Woo, J.-H., He, K., Lu, Z., et al. (2017). MIX: a mosaic Asian anthropogenic emission inventory under the international collaboration framework of the MICS-Asia and HTAP. *Atmospheric Chemistry and Physics, 17*(2), https://doi.org/10.5194/acp-17-935-2017

Liao, F., Su, R., Chan, P.-W., Qi, Y., & Hon, K.-K. (2019). Observational Study on the Characteristics of the Boundary Layer during Changes in the Intensity of Tropical Cyclones Landing in Guangdong, China. Advances in Meteorology, 2019, 8072914. https://doi.org/10.1155/2019/8072914

Lin, M., Oki, T., Bengtsson, M., Kanae, S., Holloway, T., & Streets, D. G. (2008). Long-range transport of acidifying substances in east Asia - Part II - Source-receptor relationships. *Atmospheric Environment, 42*(24), https://doi.org/10.1016/j.atmosenv.2008.03.039

Lin, T. C., Hamburg, S. P., King, H. B., & Hsia, Y. J. (2000). Throughfall patterns in a subtropical rain forest of northeastern Taiwan. *Journal of Environmental Quality, 29*(4), https://doi.org/10.2134/jeq2000.00472425002900040022x

Lu, Z., & Streets, D. G. (2012). Increase in NOx Emissions from Indian Thermal Power Plants during 1996–2010: Unit-Based Inventories and Multisatellite Observations. *Environmental Science & Technology, 46*(14), https://doi.org/10.1021/es300831w

Lu, Z., Zhang, Q., & Streets, D. G. (2011). Sulfur dioxide and primary carbonaceous aerosol emissions in China and India, 1996–2010. *Atmospheric Chemistry and Physics, 11*(18), https://doi.org/10.5194/acp-11-9839-2011

MERK (Ministry of Environment, R. o. K. (2019). *Environmental Statistics Yearbook*. Retrieved from https://library.me.go.kr/#/search/detail/5691985?offset=1#btn-export

Merrill, R. T. (1984). A Comparison of Large and Small Tropical Cyclones. *Monthly Weather Review, 112*(7), https://doi.org/10.1175/1520-0493(1984)112<1408:Acolas>2.0.Co;2

Okin, G. S., Baker, A. R., Tegen, I., Mahowald, N. M., Dentener, F. J., Duce, R. A., et al. (2011). Impacts of atmospheric nutrient deposition on marine productivity: Roles of nitrogen, phosphorus, and iron. *Global Biogeochemical Cycles, 25*(2), https://doi.org/10.1029/2010gb003858

Okita, T., Hara, H., & Fukuzaki, N. (1996). Measurements of atmospheric SO2 and SO42-, and determination of the wet scavenging coefficient of sulfate aerosols for the winter monsoon season over the Sea of Japan. *Atmospheric Environment, 30*(22), https://doi.org/10.1016/1352-2310(96)00090-8

Page, T., Whyatt, J. D., Metcalfe, S. E., Derwent, R. G., & Curtis, C. (2008). Assessment of uncertainties in a long range atmospheric transport model: Methodology, application and implications in a UK context. Environ Pollut, 156(3), 997-1006. https://www.ncbi.nlm.nih.gov/pubmed/18572287

Palmer, P. I., Abbot, D. S., Fu, T.-M., Jacob, D. J., Chance, K., Kurosu, T. P., et al. (2006). Quantifying the seasonal and interannual variability of North American isoprene emissions using satellite observations of the formaldehyde column. *Journal of Geophysical Research, 111*(D12), https://doi.org/10.1029/2005jd006689

Pitcairn, C. E., Fowler, D., Leith, I. D., Sheppard, L. J., Sutton, M. A., Kennedy, V., & Okello, E. (2003). Bioindicators of enhanced nitrogen deposition. Environ Pollut, 126(3), 353-361. https://www.ncbi.nlm.nih.gov/pubmed/12963296

Qu, Y., An, J., He, Y., & Zheng, J. (2016). An overview of emissions of SO2 and NOx and the long-range transport of oxidized sulfur and nitrogen pollutants in East Asia. *J Environ Sci (China), 44*, https://doi.org/10.1016/j.jes.2015.08.028

Qu, Y., Chen, B. J., Ming, J., Lynn, B. H., & Yang, M. J. (2017). Aerosol Impacts on the Structure, Intensity, and Precipitation of the Landfalling Typhoon Saomai (2006). *Journal of Geophysical Research-Atmospheres, 122*(21), https://doi.org/10.1002/2017jd027151

Rastogi, N., & Sarin, M. M. (2005). Chemical characteristics of individual rain events from a semi-arid region in India: Three-year study. *Atmospheric Environment, 39*(18), https://doi.org/10.1016/j.atmosenv.2005.01.053

Sakihama, H., & Tokuyama, A. (2005). Effect of typhoon on chemical composition of rainwater in Okinawa Island, Japan. *Atmospheric Environment, 39*(16), https://doi.org/10.1016/j.atmosenv.2004.12.043

Sanderson, M. G., Dentener, F. J., Fiore, A. M., Cuvelier, C., Keating, T. J., Zuber, A., et al. (2008). A multi-model study of the hemispheric transport and deposition of oxidised nitrogen. *Geophysical Research Letters, 35*(17), https://doi.org/10.1029/2008gl035389

Santachiara, G., Prodi, F., & Belosi, F. (2012). A Review of Termo- and Diffusio-Phoresis in the Atmospheric Aerosol Scavenging Process. Part 1: Drop Scavenging. *Atmospheric and Climate Sciences, 02*(02), https://doi.org/10.4236/acs.2012.22016

Saylan, L., Toros, H., & Sen, O. (2009). Back Trajectory Analysis of Precipitation Chemistry in the Urban and Forest Areas of Istanbul, Turkey. *Clean-soil Air Water, 37*(2), https://doi.org/10.1002/clen.200800001

Seinfeld, J. H., & Pandis, S. N. (2016). *Atmospheric Chemistry and Physics: From air pollution to climate change*.

Shen, J., Chen, D., Bai, M., Sun, J., Coates, T., Lam, S. K., & Li, Y. (2016). Ammonia deposition in the neighbourhood of an intensive cattle feedlot in Victoria, Australia. *Sci Rep, 6*, https://doi.org/10.1038/srep32793

Skamarock, W., Klemp, J., Dudhia, J., Gill, D., Barker, D., Duda, M., et al. (2008). *A Description of the Advanced Research WRF Version 3*.

Tan, J. N., Fu, J. S., Dentener, F., Sun, J., Emmons, L., Tilmes, S., et al. (2018). Multi-model study of HTAP II on sulfur and nitrogen deposition. *Atmospheric Chemistry and Physics, 18*(9), https://doi.org/10.5194/acp-18-6847-2018

Tian, Y., Wang, Z., Pan, X., Li, J., Yang, T., Wang, D., et al. (2020). Influence of the morphological change in natural Asian dust during transport: A modeling study for a typical dust event over northern China. *Sci Total Environ, 739*, https://doi.org/10.1016/j.scitotenv.2020.139791

Toyonaga, S., & Zhang, D. (2016). Wet Deposition Fluxes of Ions Contributed by Cyclone-, Stationary Front- and Typhoon-associated Rains at the Southwestern Japan Coast. *Asian Journal of Atmospheric Environment, 10*(2), https://doi.org/10.5572/ajae.2016.10.2.057

Van Damme, M., Clarisse, L., Whitburn, S., Hadji-Lazaro, J., Hurtmans, D., Clerbaux, C., & Coheur, P.-F. (2018). Industrial and agricultural ammonia point sources exposed. *Nature, 564*(7734), https://doi.org/10.1038/s41586-018-0747-1

Wang, J., Yu, Z., Wei, Q., & Yao, Q. (2019). Long-Term Nutrient Variations in the Bohai Sea Over the Past 40 Years. Journal of Geophysical Research: Oceans, 124(1), 703-722.

Wang, Z., Itahashi, S., Uno, I., Pan, X., Osada, K., Yamamoto, S., et al. (2017). Modeling the long-range transport of particulate matters for january in East Asia using NAQPMS and CMAQ. *Aerosol and Air Quality Research, 17*, https://doi.org/10.4209/aaqr.2016.12.0534

Wang, Z. F., Maeda, T., Hayashi, M., Hsiao, L. F., & Liu, K. Y. (2001). A nested air quality prediction modeling system for urban and regional scales: Application for high-ozone episode in Taiwan. *Water Air and Soil Pollution, 130*(1-4), https://doi.org/10.1023/A:1013833217916

Webster, P. J., Curry, J. A., Liu, J., & Holland, G. J. (2006).

Response to comment on "Changes in tropical cyclone number, duration, and intensity in a warming environment". *Science, 311*(5768), https://doi.org/10.1126/science.1121564

Wesely, M. (2007). Parameterization of surface resistances to gaseous dry deposition in regional-scale numerical models☆. *Atmospheric Environment, 41*, https://doi.org/10.1016/j.atmosenv.2007.10.058

Whitburn, S., Van Damme, M., Kaiser, J. W., van der Werf, G. R., Turquety, S., Hurtmans, D., et al. (2015). Ammonia emissions in tropical biomass burning regions: Comparison between satellite-derived emissions and bottom-up fire inventories. *Atmospheric Environment, 121*, https://doi.org/10.1016/j.atmosenv.2015.03.015

Wu, J. B., Wang, Z., Wang, Q., Li, J., Xu, J., Chen, H., et al. (2017). Development of an on-line source-tagged model for sulfate, nitrate and ammonium: A modeling study for highly polluted periods in Shanghai, China. *Environ Pollut, 221*, https://doi.org/10.1016/j.envpol.2016.11.061

Wu, Q. Z., Wang, Z. F., Gbaguidi, A., Gao, C., Li, L. N., & Wang, W. (2011). A numerical study of contributions to air pollution in Beijing during CAREBeijing-2006. *Atmos. Chem. Phys., 11*(12), https://doi.org/10.5194/acp-11-5997-2011

Xu, D. (2020). *The study of below-cloud wet scavenging mechanism for aerosols and its numerical simulation.* (Doctoral dissertation), University of Chinese Academy of Sciences, Retrieved from Dissertation knowledge discovery system. Location: Institute of Atmospheric Physics.

Xu, D., Ge, B., Wang, Z., Sun, Y., Chen, Y., Ji, D., et al. (2017). Below-cloud wet scavenging of soluble inorganic ions by rain in Beijing during the summer of 2014. *Environ Pollut, 230*, https://doi.org/10.1016/j.envpol.2017.07.033

Xu, D. H., Ge, B. Z., Chen, X. S., Sun, Y. L., Cheng, N. L., Li, M., et al. (2019). Multi-method determination of the below-cloud wet scavenging coefficients of aerosols in Beijing, China. *Atmospheric Chemistry and Physics, 19*(24), https://doi.org/10.5194/acp-19-15569-2019

Yamagata, S., Kobayashi, D., Ohta, S., Murao, N., Shiobara, M., Wada, M., et al. (2009). Properties of aerosols and their wet deposition in the arctic spring during ASTAR2004 at Ny-Alesund, Svalbard. *Atmospheric Chemistry and Physics, 9*(1), https://doi.org/10.5194/acp-9-261-2009

Yan, J., Chen, L., Lin, Q., Zhao, S., & Zhang, M. (2016). Effect of typhoon on atmospheric aerosol particle pollutants accumulation over Xiamen, China. *Chemosphere, 159*, https://doi.org/10.1016/j.chemosphere.2016.06.006

Yang, W., Li, J., Wang, M., Sun, Y., & Wang, Z. (2018). A Case Study of Investigating Secondary Organic Aerosol Formation Pathways in Beijing using an Observation-based SOA Box Model. *Aerosol and Air Quality Research, 18*, https://doi.org/10.4209/aaqr.2017.10.0415

Zhang, J., Zhang, Z. F., Liu, S. M., Wu, Y., Xiong, H., & Chen, H. T. (1999). Human impacts on the large world rivers: Would the Changjiang (Yangtze River) be an illustration? *Global Biogeochemical Cycles, 13*(4), https://doi.org/10.1029/1999gb900044

Zheng, B., Geng, G., Ciais, P., Davis, S., Martin, R., Meng, J., et al. (2020). Satellite-based estimates of decline and rebound in China's CO2 emissions during COVID-19 pandemic. *Science Advances, 6*, https://doi.org/10.1126/sciadv.abd4998

Zhou, Y., Wang, T., Gao, X., Xue, L., Wang, X., Wang, Z., et al. (2010). Continuous observations of water-soluble ions in PM2.5 at Mount Tai (1534 m a.s.l.) in central-eastern China. Journal of Atmospheric Chemistry, 64(2-3), https://doi.org/10.1007/s10874-010-9172-z

IOP Publishing Journal Title
Journal **XX** (XXXX) XXXXXX https://doi.org/XXXX/XXXX

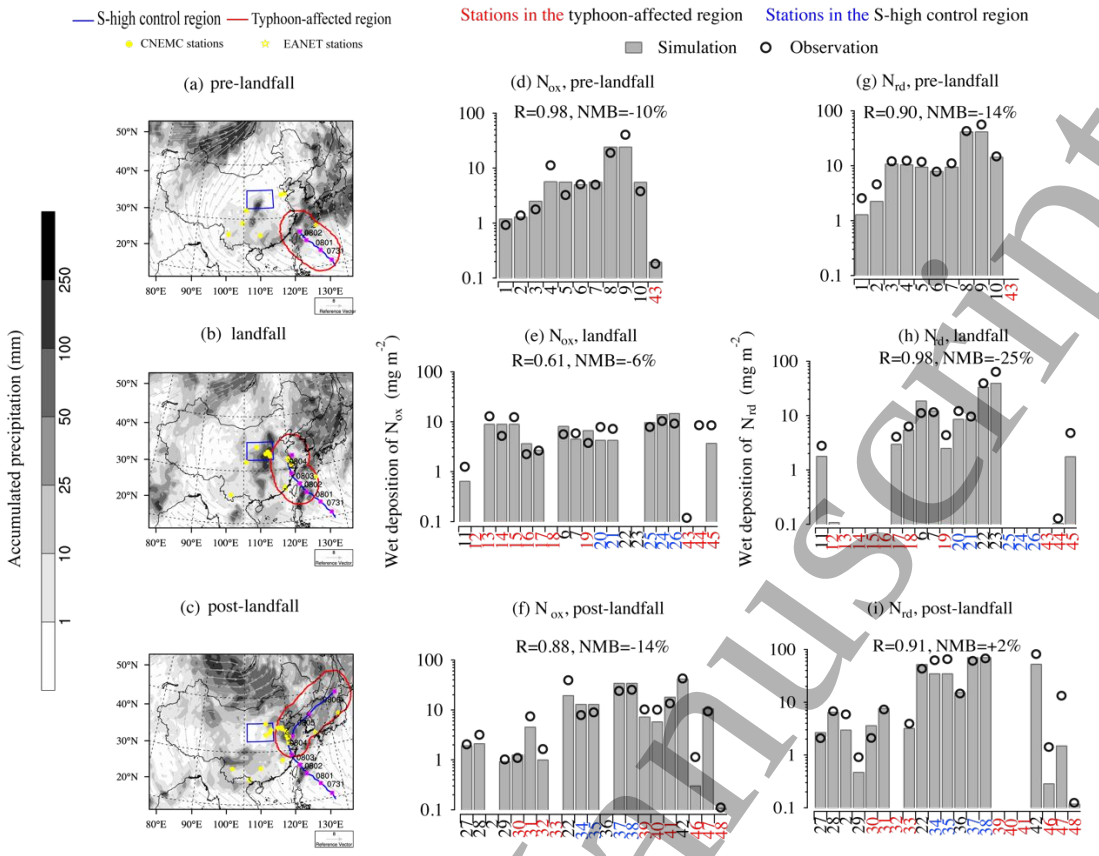

Figure 1. Comparison between observed (circles) and simulated (bars) wet deposition of (a–c) N_{ox} and (d–f) N_{rd} during the pre-landfall (1–2 August), landfall (3–4 August) and post-landfall (5–6 August) stages. The stations are numbered and listed in order from south to north. The locations and characteristics of the stations can be referred to in Table S2. The statistical parameters, i.e., *R* and NMB, are shown in the inset, and their formulae can be referred to in Table S6.

IOP Publishing Journal Title
Journal **XX** (XXXX) XXXXXX https://doi.org/XXXX/XXXX

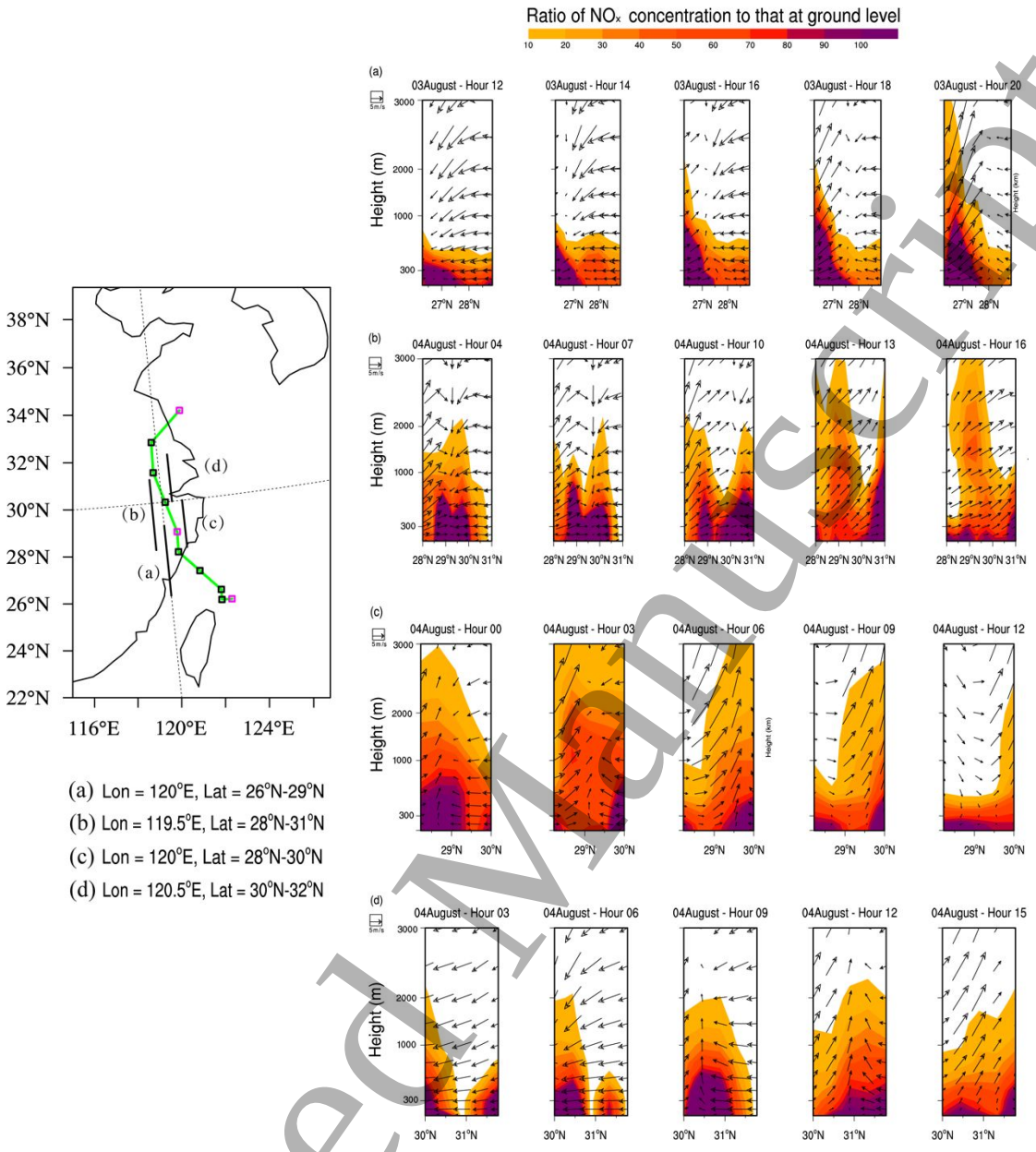

Figure 2. Latitude–height cross sections of the ratio of the NO_x concentration to that at ground level with the vertical wind vector superimposed at (a) 120°E, 26°N–29°N; (b) 119.5°E, 28°–31°N; (c) 120°E, 28°–30°N, and (d) 120.5°E, 30°–32°N. Note that the pink boxes in the left inset represent typhoon locations at 00:00 UTC, while the black ones represent the typhoon locations every 6 h.

IOP Publishing Journal Title
Journal **XX** (XXXX) XXXXXX https://doi.org/XXXX/XXXX

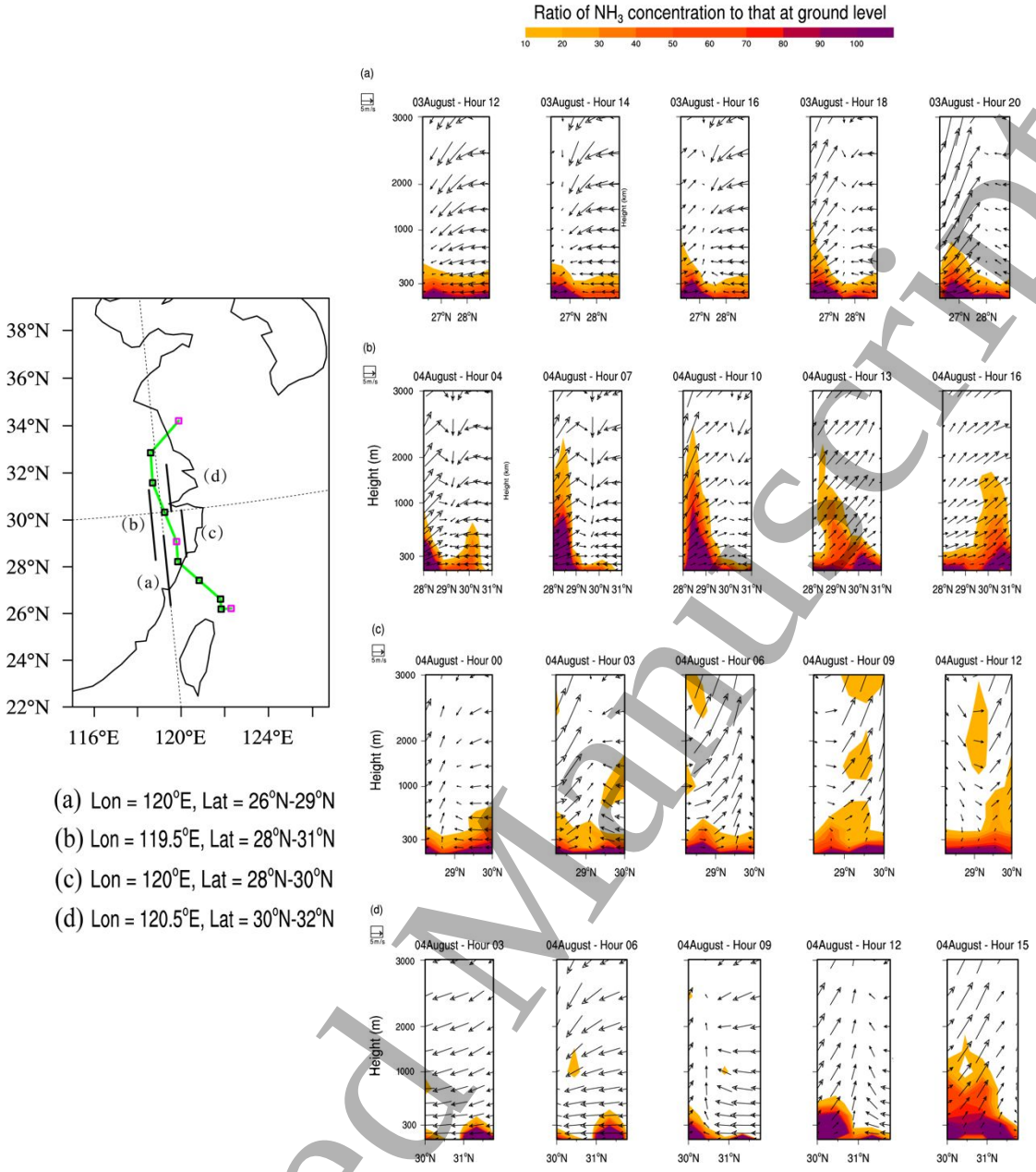

Figure 3. Same as Figure 2, but for NH_3.

IOP Publishing Journal Title
Journal **XX** (XXXX) XXXXXX https://doi.org/XXXX/XXXX

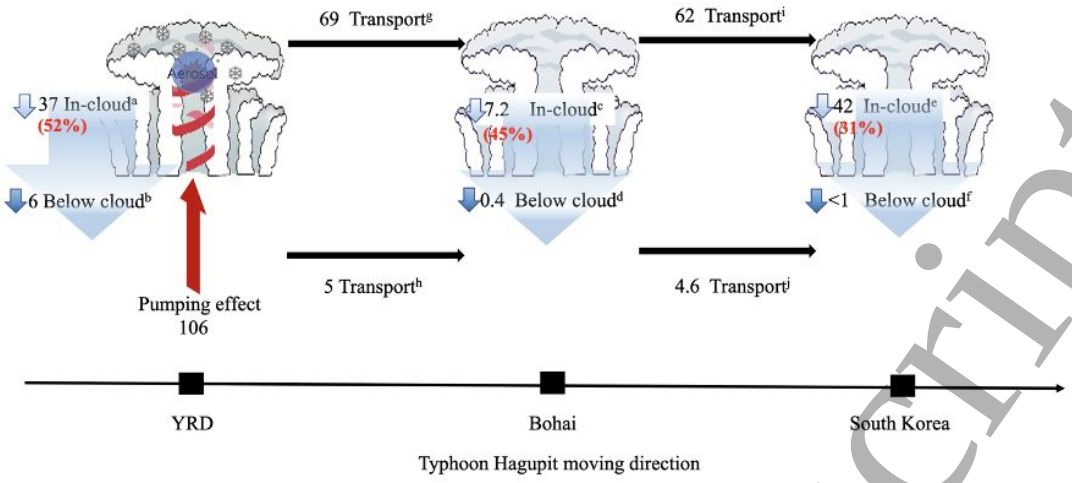

Figure 4. Schematic diagram of the 'pumping effect' which means the pumping up to the cloud of typhoon. The number (a-j) is in- or below-cloud wet deposition of N_{ox} (unit: $\times 10^{-3}$ mg m^{-2}) while that in parentheses and red are the in-cloud contributions from YRD (unit: %).

IOP Publishing Journal Title
Journal **XX** (XXXX) XXXXXX https://doi.org/XXXX/XXXX

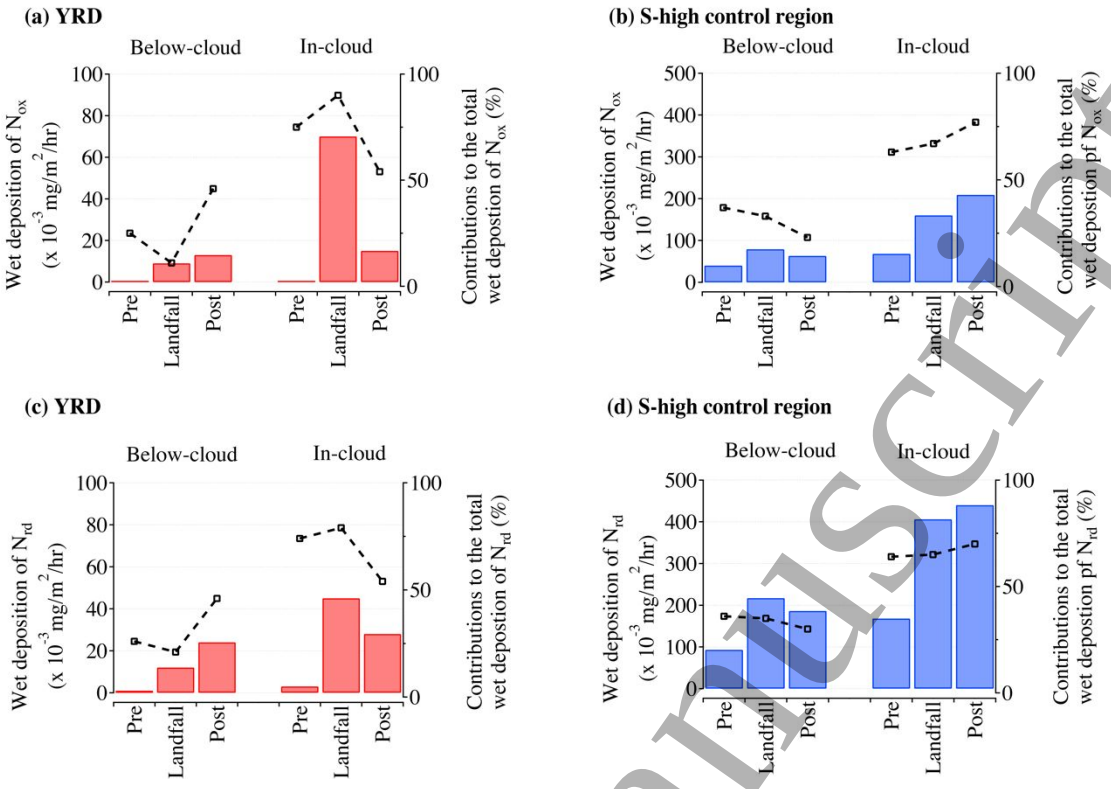

Figure 5. Box plots of below-cloud and in-cloud wet deposition and corresponding contributions to total wet deposition of N_{ox} or N_{rd} during the pre-landfall (1–2 August), landfall (3–4 August) and post-landfall (5–6 August) stages in the (a, c) YRD and (b, d) S-high control region.

IOP Publishing Journal Title
Journal **XX** (XXXX) XXXXXX https://doi.org/XXXX/XXXX

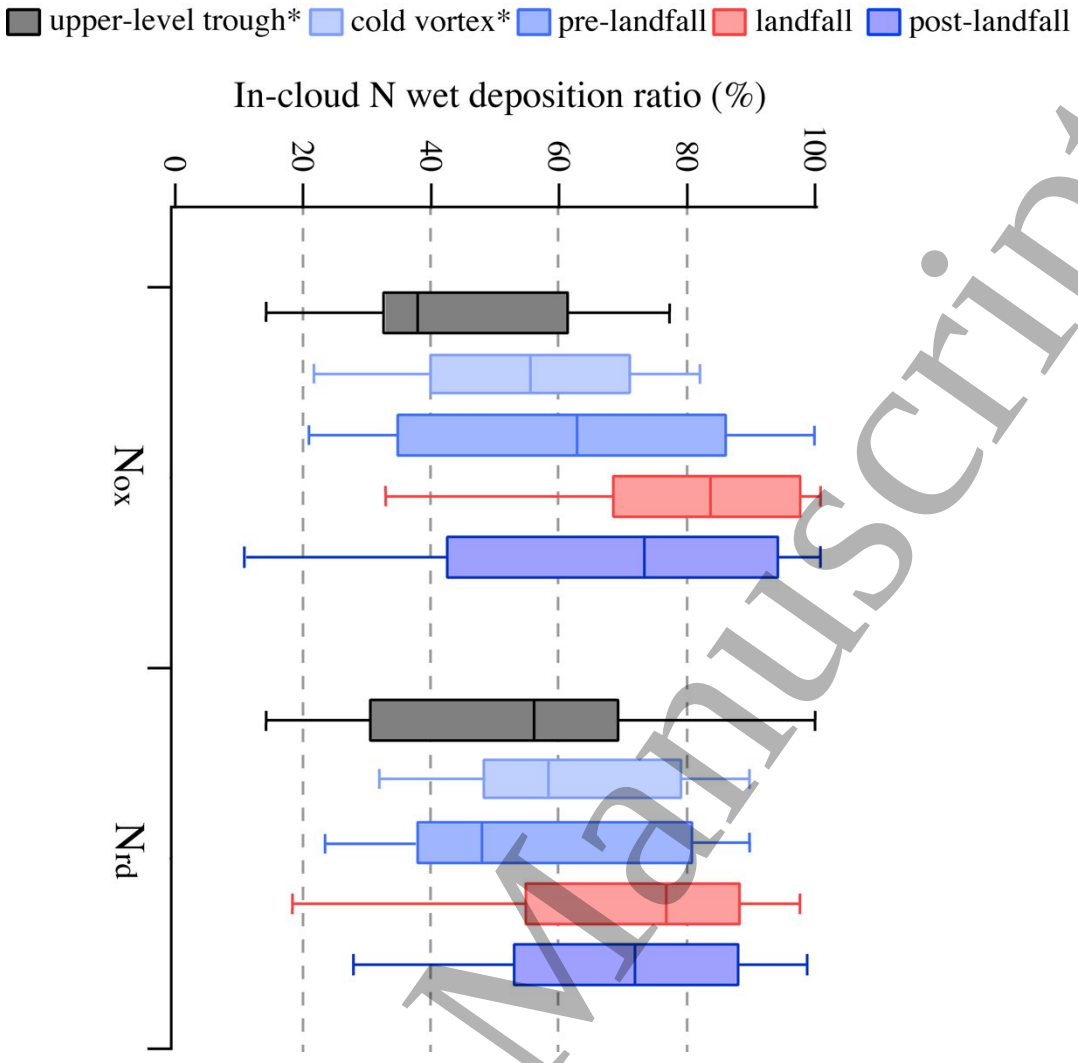

Figure 6. in-cloud wet deposition contributions of N_{ox} and N_{rd} for upper-level trough, cold vortex and three different typhoon stages (pre-landfall (1-2 August), landfall (3-4 August) and post-landfall (5-6 August)). Note that the two observation results i.e. upper-level trough and cold vortex marked with stars are derived from Ge et al., 2021.

IOP Publishing Journal Title
Journal **XX** (XXXX) XXXXXX https://doi.org/XXXX/XXXX

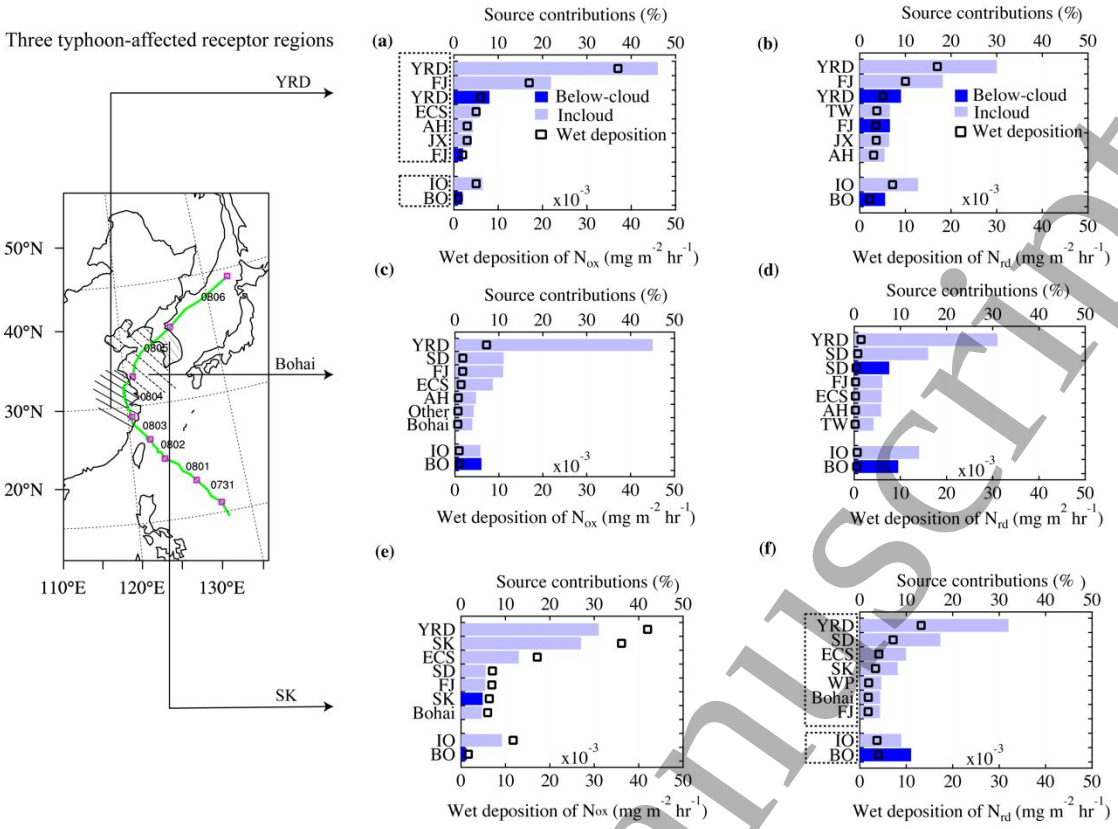

Figure 7. Source contributions to the in-cloud (light blue) and below-cloud (dark blue) wet deposition of N_{ox} (left) and N_{rd} (right) when typhoon Hagupit made landfall in three typhoon-affected receptor regions: (a, b) SK, (c, d) Bohai; (e, f) YRD. The left-hand coordinate is the abbreviation of the source region, which can be referred to in Figure S1. Except for the top seven sources regions in terms of source contributions, the rest are replaced with IO and BO, which represents other sources of in-cloud and below-cloud, respectively. Note that the pink boxes in the left-hand inset represents the typhoon locations at 00:00 UTC, while the green line represents the 6-hourly typhoon track.

